RADIOTRONICS

Vol. 28, No. 8 August, 1963

8

IN THIS ISSUE

AN AWV PUBLICATION

REGISTERED IN AUSTRALIA FOR TRANSMISSION BY POST AS A PERIODICAL.

SOLID-STATE PHOTOCELLS

Introduction

Among the many new devices that semiconductor theory has brought us is the solid-state photocell, which is rapidly assuming a prominent position in the field of devices that are sensitive to light and other forms of electromagnetic radiation. There are many materials and arrangements of materials which are sensitive to electromagnetic radiation, but only a few of them appear to have any commercial importance; that is, only a few of them exhibit the required characteristics to a degree that warrants practical exploitation. The most important materials from a practical point of view are cadmium-sulphide, germanium and silicon, and cells employing these materials will be described here.

It is proposed to deal with two basic types of photosensitive devices, the photoconductive cell and the photojunction cell. From the commercial viewpoint, both of these types may be further subdivided.

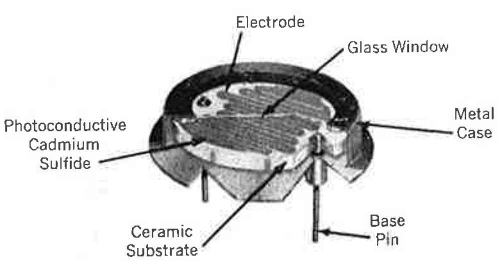

Fig. 1—Cutaway view of a typical CdS photoconductive cell.

Photoconductive cells use a photoconductive material, that is, one in which the electrical resistance, and therefore the flow of charge carriers, is a function of the incident electromagnetic radiation. These cells may be divided for the purpose of classification into broad-area types, or those which use a polycrystalline photosensitive surface, and the single-crystal types.

Broad-area photoconductive cells are characterized by high sensitivity to visible radiation and moderate speed of response to changes in illumination. They are used extensively in control circuits where changes in incident light are required to operate relays directly without the aid of amplifiers, in punched-card reading, automatic iris controls in cameras, automatic street lighting control, and similar applications.

The single-crystal type of photoconductive cell has good sensitivity, moderate speed of response, and is used in applications where a very sharp spectral response in the blue-green region of the visible spectrum is required.

Photojunction cells, as the name implies, consist of a p-n semiconductor junction which is sensitive to incident radiation. In this case, however, instead of the incident energy changing the resistance of the material, and consequently the current flowing through it, the junction is used to convert the incident energy directly into electrical power. It is one of a number of direct energy conversion systems.

Commercially-important photojunction cells may be subdivided into germanium p-n alloy

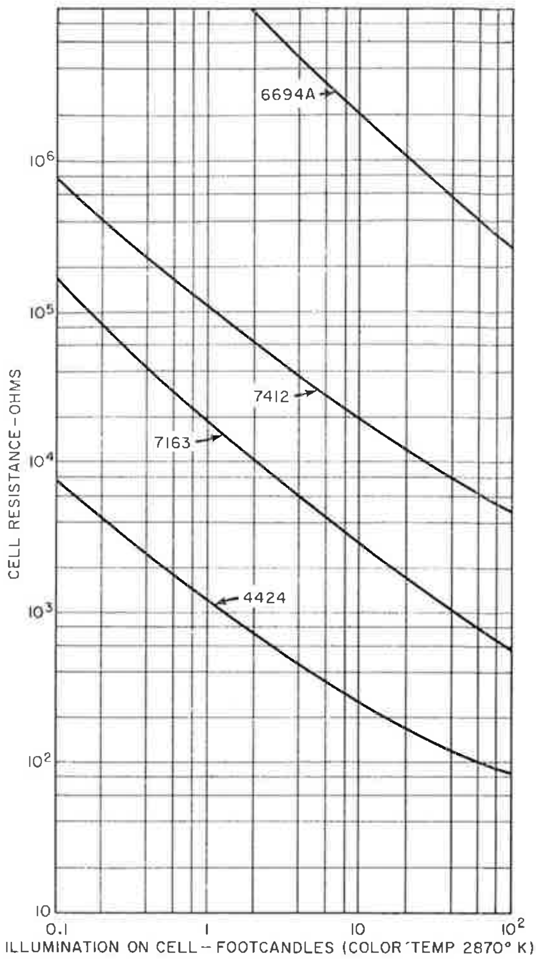

Fig. 2—DC cell resistance as a function of cell illumination for some typical photoconductive cells.

types, and the silicon photovoltaic cells. The Ge p-n junction cells have good sensitivity, and a speed of response to changing light signals that is well beyond the audio range. This type of cell is recommended for the high-speed reading of punched cards and tape, and in sound pickup from motion-picture film. Silicon voltaic cells are used primarily for the direct conversion of solar radiant energy into electrical power, and in light measuring and light-operated control applications. They have good stability, and do not require an external power supply.

Broad-area CdS Photoconductive Cells

The essential elements of a cadmium-sulphide photocell are a ceramic substrate, a layer of photoconductive cadmium sulphide, electrodes, and a protective moisture-resistant enclosure. A cutaway view of a typical glass-metal photoconductive cell is shown in Fig. 1.

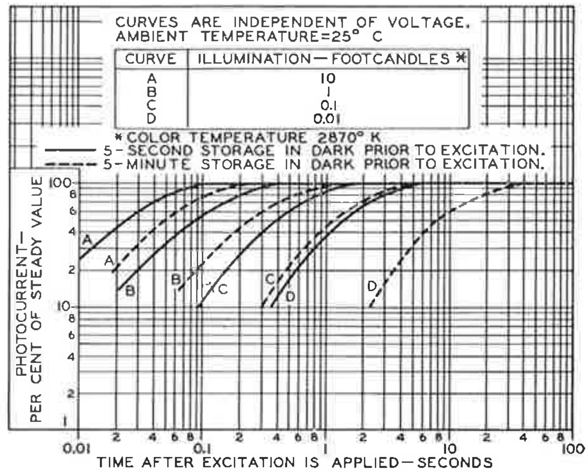

Fig. 3—Typical rise characteristics of a CdS cell.

The cadmium sulphide is treated (doped) with various activating materials, such as chloride and copper, for increased sensitivity. The electrodes are formed by evaporation of a metal through a mask. Tin, indium, and gold are commonly used electrode metals although the latter results in non-ohmic contacts, i.e., rectifying contacts between the electrode metal and the cadmium sulphide. Envelopes of plastic materials are used at times, but glass and glass-metal enclosures are generally required for applications in which high humidity may be encountered.

Cadmium-sulphide photoconductive cells having ohmic contacts behave in a circuit as an ohmic impedance. One of the most important parameters of the photocell is its resistance at different levels of illumination. DC cell resistance as a function

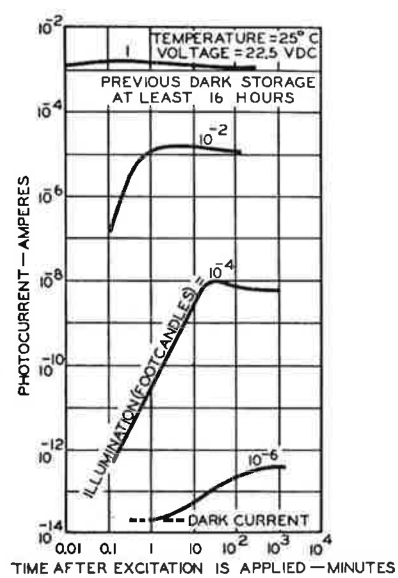

Fig. 4—Rise characteristics of a CdS cell selected for low dark current.

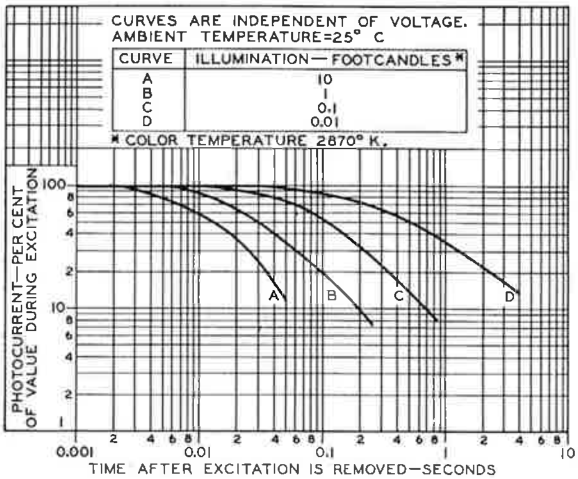

Fig. 5—Typical decay characteristics of a CdS cell.

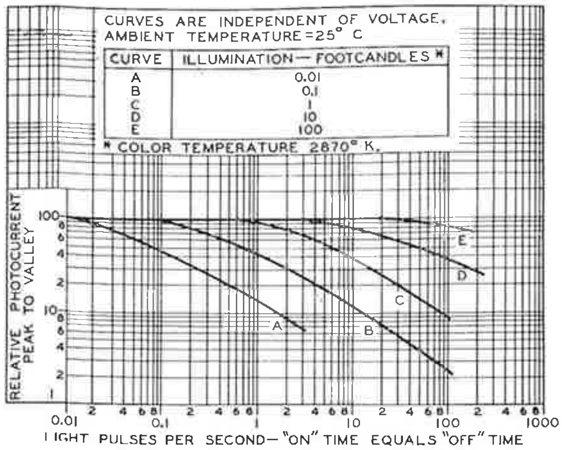

Fig. 7—Response characteristics of a CdS cell to pulsed light.

of cell illumination for some typical photoconductive cells is shown in Fig. 2. It will be noted that the slope of the curves varies slowly and is nearly constant about any given operating point. Resistance may be expressed as

$$R_1 L^{-\gamma}$$

where R_1 is the resistance of the cell in ohms per unit illumination
L is the illumination in footcandles, and
γ is the slope of the characteristic at a given operating point

The performance of a photocell at a given operating point is described by specifying R_1 and γ. For a typical cell, the 7163, R_1 and γ are 0.019×10^6 ohms and 1, respectively (at 1 footcandle). The resistance or conductance of the cell is often indirectly expressed in terms of the current drawn through the cell at a given voltage and given light level.

The conductance (1/resistance) of this type of cell does not change rapidly with changes in incident illumination but requires some time to reach its steady-state value. This effect results from the presence of electron traps within the forbidden region of the band gap of the cadmium sulphide. Although the build-up and decay of conductance and current upon the application or removal of illumination is only approximately exponential, the term "time constant" is frequently used to describe the time required for conductance or current to reach 63.2% (rise) or 36.8% (fall) of its maximum value. If a photoconductive cell has been stored in the dark for a long period of time

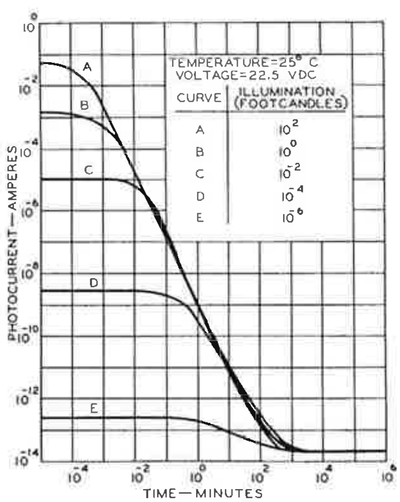

Fig. 6—Decay characteristics of a CdS cell selected for low dark current.

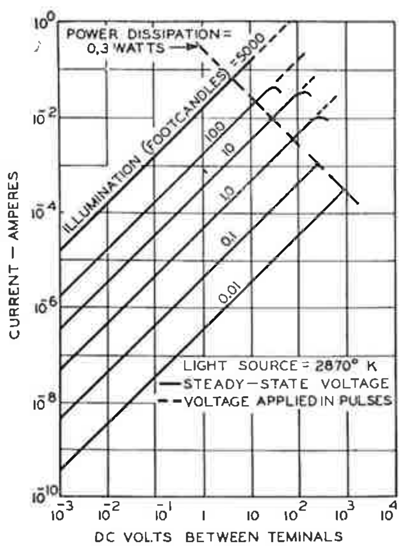

Fig. 8—Current versus voltage characteristics of a CdS cell.

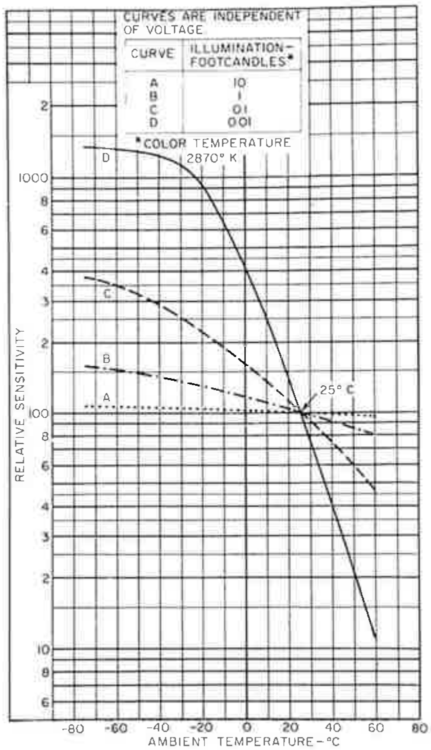

Fig. 9—Typical characteristics of a CdS cell.

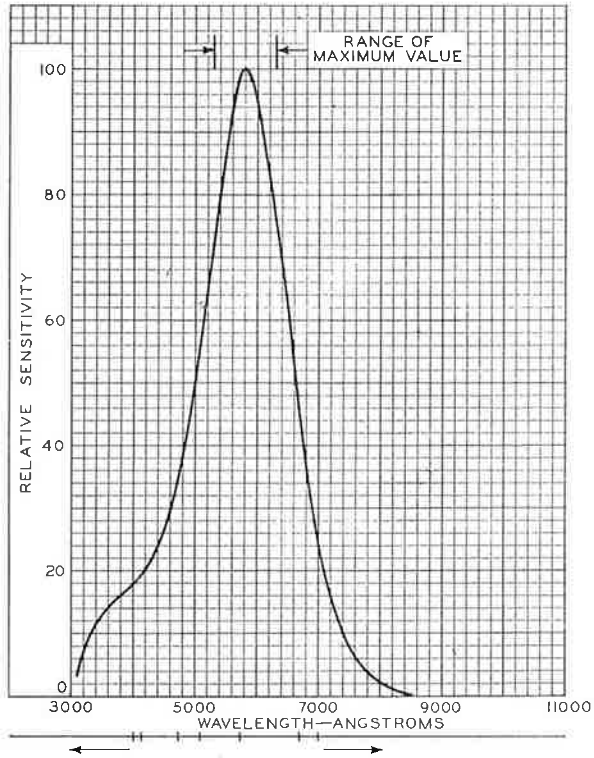

Fig. 10—Tentative spectral sensitivity characteristic for a CdS cell, S15 response. The curve is shown for equal values of radiant flux at all wavelengths.

and is suddenly illuminated with 10 footcandles of illumination, its time constant is approximately 70 milliseconds. The time constant depends on the intensity of the applied illumination. In general, the cell responds more quickly to high illumination light levels than to low light levels and its rise time is usually longer than its decay time. Photocurrent rise curves are shown in Fig. 3 and Fig. 4.

In addition to these time effects, there are other time-associated phenomena that take place more slowly. These phenomena can best be described by saying that the cell has some memory of previous light exposure. Long exposure to high light levels tends to make the cell slightly less sensitive and somewhat faster in response regardless of whether or not voltage is applied to the cell during exposure. These changes are reversible, and the cell will revert to its former condition after a storage period in the dark.

Because of the "memory" of the photocell, it is desirable to "light-precondition" a cell before a measurement of photocurrent is made. A commonly used preconditioning schedule employed in production testing is the exposure of the cell for 16 to 24 hours to 500 footcandles of fluorescent light. Voltage is not applied to the cell during the preconditioning schedule.

There are also time effects related to the application of voltage. For example, a cell is slightly less sensitive under ac voltage operation than under dc voltage operation.

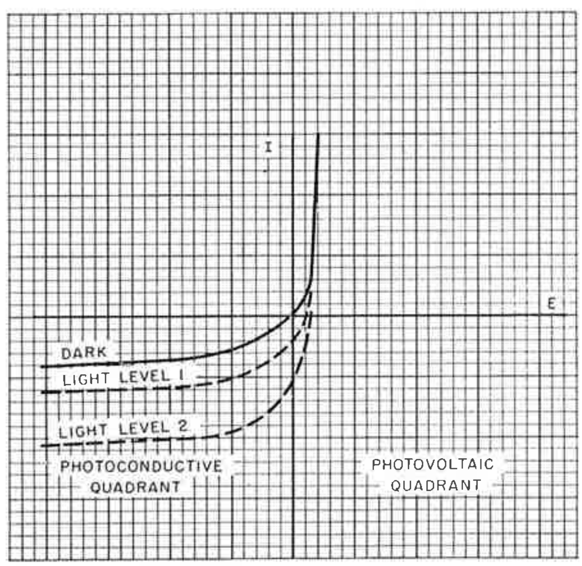

Fig. 11—Current versus voltage characteristics for a junction photodevice.

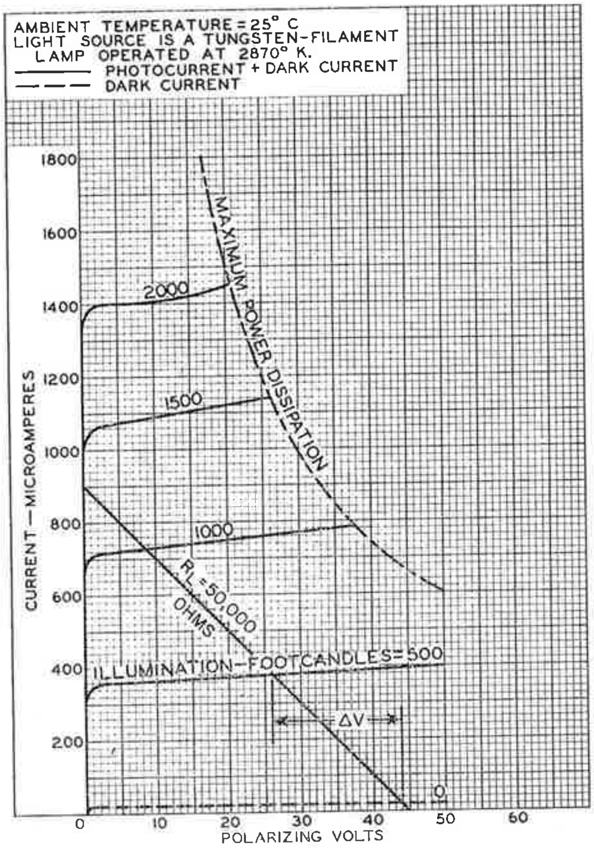

Fig. 12—Typical characteristics of Ge p-n alloy photojunction cells.

In most photocell applications, it is important that the conductance of the cell be substantially less when the cell is in the dark than when it is illuminated. The terms dark current and decay current are used to describe cell performance under un-illuminated conditions. Dark current is that current which passes through the cell under specified conditions of voltage and temperature after the cell has been in the dark for a long period of time. Dark current usually has a very low value. Because of the time effects, it is more convenient to specify the decay current which is observed at a given time interval following the removal of a given level of illumination. For the 7163 at an applied voltage of 50 volts, decay current is below 40 μa, 10 seconds after the removal of 1 footcandle of illumination. Photocurrent decay curves are shown in Fig. 5 and Fig. 6.

Peak-to-valley response as a function of square-wave light input for a typical cell is shown in Fig. 7. As expected, the frequency response is higher for higher levels of illumination.

A typical family of curves showing photocurrent as a function of applied voltage at different levels of illumination is shown in Fig. 8. Linearity extends over six orders of magnitude.

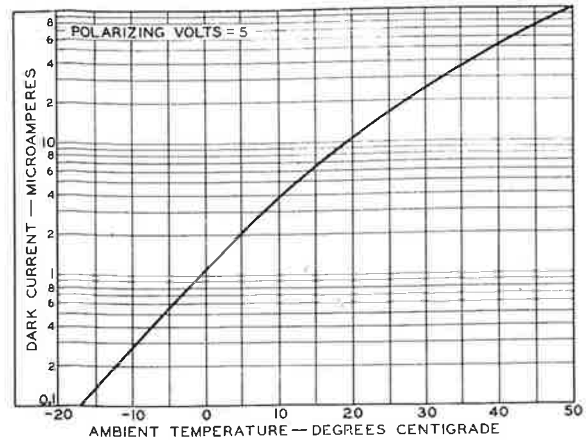

Fig. 13—Typical dark-current characteristic of Ge p-n alloy photojunction cells.

The sensitivity of the cell tends to decrease as ambient temperature rises; typical curves are shown in Fig. 9. The effect is marked at low levels of illumination but tends to become insignificant at 10 footcandles and higher.

The sensitivity of the photocell is also dependent on the wavelength of incident illumination, as shown in Fig. 10. The response curve, which is centred well within the visible spectrum, has a peak of sensitivity near 5,800 angstroms. Because the spectral response of cadmium-sulphide photocells closely matches the response of the human eye, these cells are especially useful for applications in which human vision is a factor. Examples of such applications are automatic street-light control, automatic yard-light control, and automatic iris-control in photographic cameras.

Photojunction Cells

As mentioned previously, both germanium and silicon are photoconductive and are used in the manufacture of junction photocells. In the pro-

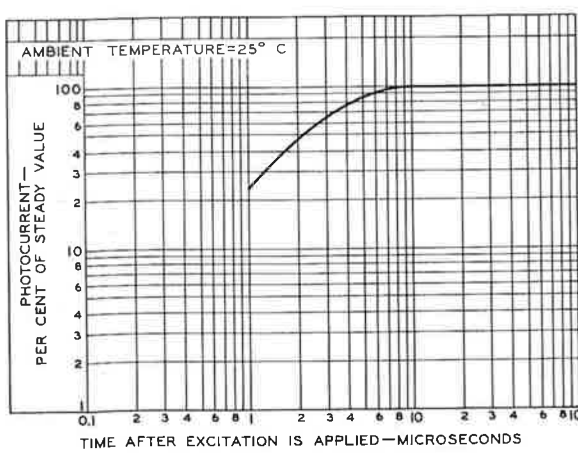

Fig. 14—Typical rise characteristic of Ge p-n alloy photojunction cells.

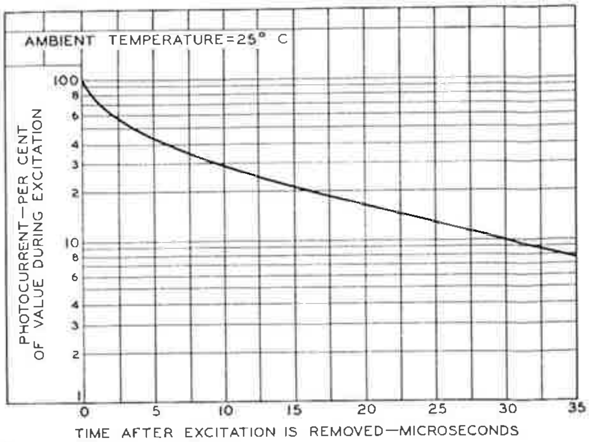

Fig. 15—Typical decay characteristic of Ge p-n alloy photojunction cells.

cessing of this type of cell, a p-n junction is formed in the material, which causes it to exhibit a non-ohmic (rectifying) characteristic, as shown in Fig. 11. The solid curve applies when the cell is in the dark; when light is applied to the cell, the curve shifts downward.

The junction photocell is customarily used as either a photoconductive device or as a photovoltaic device. In photoconductive applications, the cell is biased in the backward direction and the output voltage is developed across a series

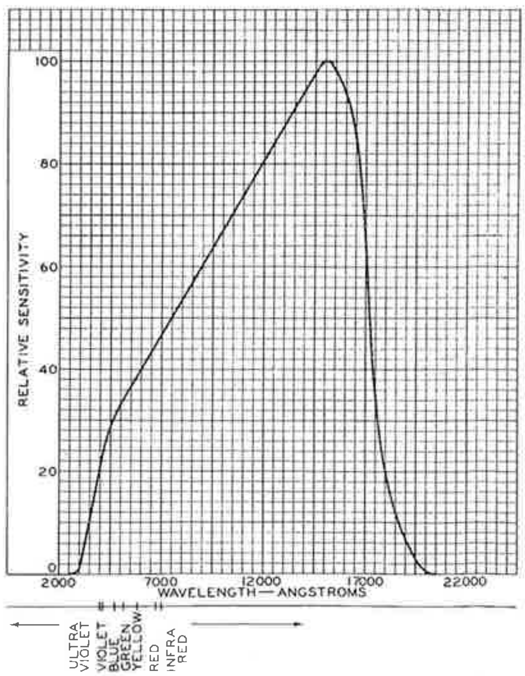

Fig. 16—Tentative spectral sensitivity characteristic for a Ge p-n alloy photojunction cell, S14 response. The curve is shown for equal values of radiant flux at all wavelengths.

load resistor. In photovoltaic applications, the cell is used to convert radiant power directly into electrical power.

Germanium p-n Alloy Photocells

When the photojunction cell is operated in the photoconductive mode, the characteristic of Fig. 11 is rotated by 180° and appears as shown in Fig. 12. A load line has been drawn for a supply voltage of 45 volts and a load resistor of 50 kilohms. If the illumination on the cell is increased from 0 to 500 footcandles, the change in voltage developed across the load resistor is Δ V.

The load resistor must be selected to have a value low enough to prevent "clipping" of the output signal due to increase in dark current at the maximum operating temperature of the system. Dark current increases with increasing temperature. A curve showing dark current as a function of temperature is shown in Fig. 13.

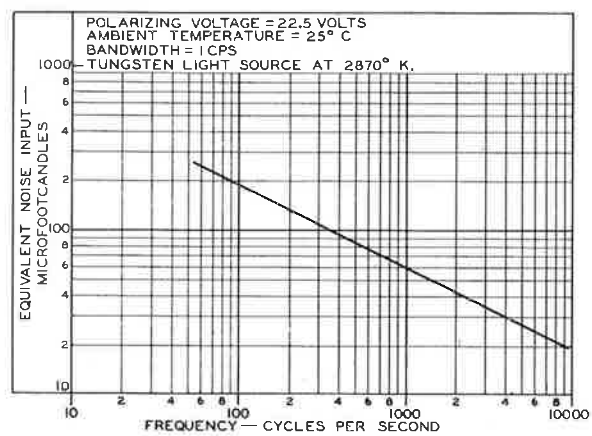

Fig. 17—Typical equivalent noise input characteristic for Ge p-n alloy photojunction cells.

The response of germanium photojunction cells to sudden changes in illumination is shown in Fig. 14 and Fig. 15. Because of its relatively fast response, the germanium photojunction cell is very useful at optical excitation frequencies well above the audio range.

Germanium photojunction cells, such as the 4420, have a quantum efficiency of approximately 0.45. Allowing for reflection from the germanium surface, one electron passes through the circuit for every photon incident on the junction. This type of photocell is thus intermediate in sensitivity between a single-unit phototube and a typical with the increase in illumination.
crease in sensitivity, i.e., photocurrent, is linear
cadmium-sulphide photoconductive cell. The in-

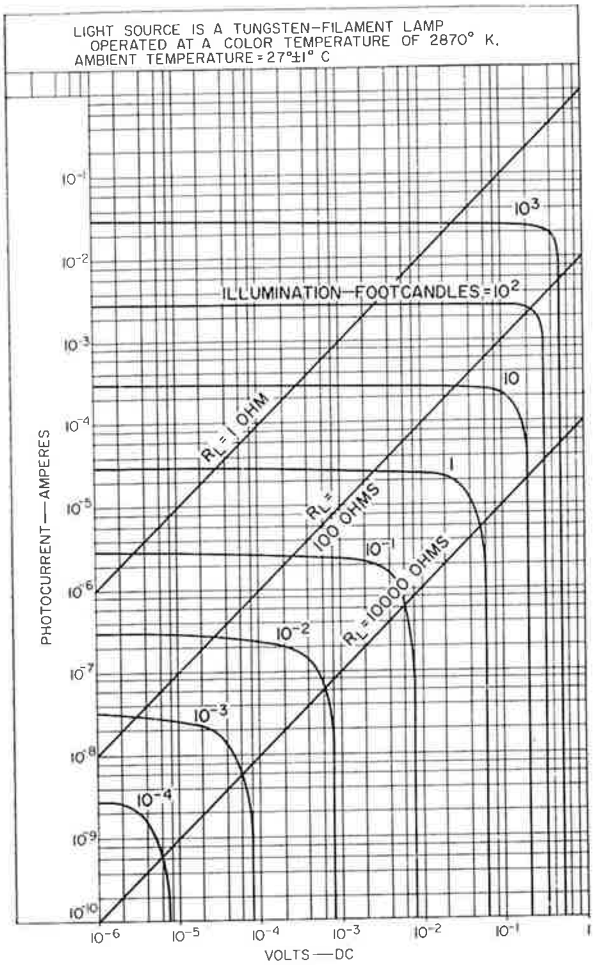

Fig. 18—Typical photocurrent-voltage relationship of n-on-p silicon photovoltaic cells.

A typical spectral response characteristic for the germanium photojunction cell is shown in Fig. 16.

The germanium photojunction cell contributes relatively low noise to a circuit. A curve of equivalent noise input is shown in Fig. 17.

Silicon Photovoltaic Cells

Cells of this type are used for converting the radiant power of the sun into electrical power. They consist of a single silicon crystal of the p-type into which a layer—about 0.5 micron thick—of an n-type material (frequently phosphorus) is diffused. The negative terminal is ordinarily a thin strip of solder which makes electrical contact with a family of metallic grid lines (electrodes). The positive terminal is usually the back surface of the cell. The n-on-p type cell is completed by applying a non-reflective coating of silicon monoxide to the front surface. This coating minimizes the reflection of useful radiant power from the silicon surface. Typical cell types are the 1cm x 2cm SL2205 and the 2cm x 2cm SL2206.

The advantage that n-on-p cells have over p-on-n cells is that they are far more resistant to degradation from the high-energy particles (protons and electrons) frequently encountered in space missions.

When the electrical performance of the silicon solar cell is analyzed, the curve of Fig. 11 is inverted to appear as shown in Fig. 18. Load lines for different series load resistors have been drawn. The value of the load resistor is usually adjusted to obtain the maximum power output from the cell for a specific condition of input illumination.

The performance of the silicon photovoltaic cell is usually described in terms of conversion efficiency which is defined as the ratio of electrical output power to incident radiant power. The load resistor is adjusted to give an output voltage of 0.46 volt, which is near the maximum power transfer point. However, care should be exercised to specify the spectral content and the intensity of the illumination in describing conversion efficiency. A typical value for conversion efficiency is between 10 and 12 per cent measured under the following conditions: the light source is a tung-

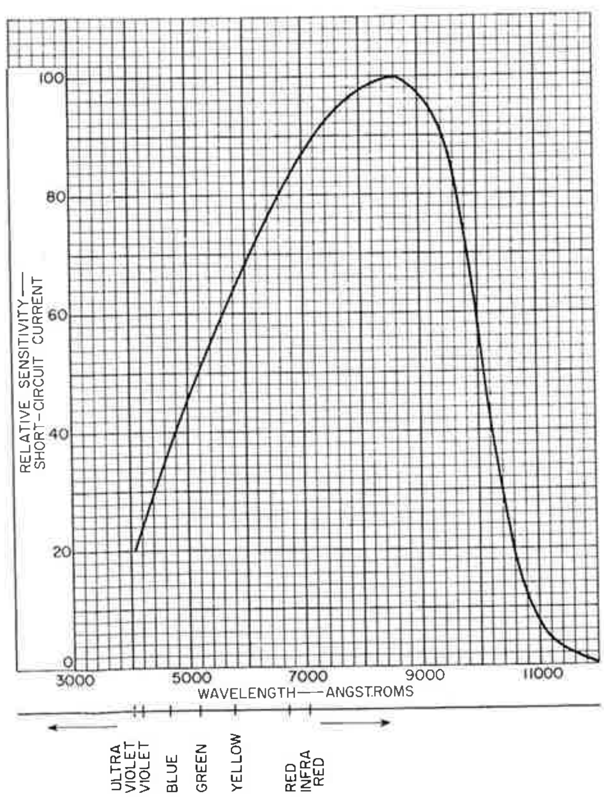

Fig. 19—Spectral sensitivity characteristic of a silicon photovoltaic cell. The curve is shown for equal values of incident flux at all wavelengths.

sten-filament lamp operated at a colour temperature of 2800°K and a water filter having a height of 1¾″ is placed between the cell and the light source. The water filter absorbs unwanted infra-red radiation. For space applications, a solar simulator which approximates the spectral output of the sun outside of the earth's atmosphere is sometimes used as the radiant energy source.

The spectral response of the silicon photovoltaic cell has its peak in the near-infrared region of the spectrum. Radiation from the sun, however, shows a peak of intensity near 4,750 angstroms. Because it is desirable, for maximum conversion efficiency, that the solar cell respond to "blue" radiation, the cell is processed in such a manner that the peak of response is shifted toward the shorter wavelengths. The shift is accomplished by making the n-layer thin (for n-on-p cells) to take advantage of the light absorption properties of the silicon. A typical response characteristic for an n-on-p cell is shown in Fig. 19.

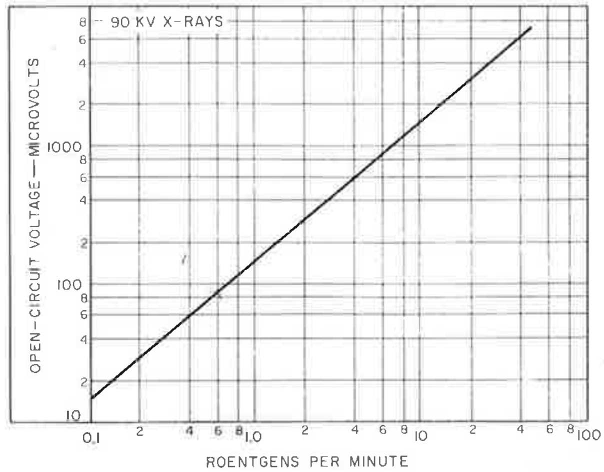

Fig. 20—X-radiation sensitivity of a silicon photovoltaic cell.

The silicon photovoltaic cell is also sensitive to X-radiation. The output of a typical cell exposed to such radiation is shown in Fig. 20.

(With acknowledgements to RCA)

USEFUL RELATED CURVES

(Useful data on lenses and photometry are given on page 155)

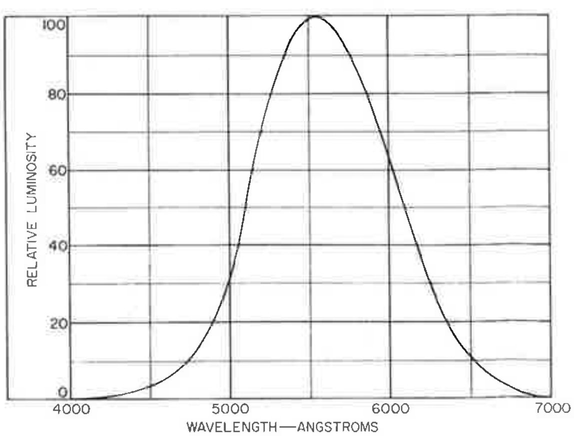

Visibility characteristic of the human eye.

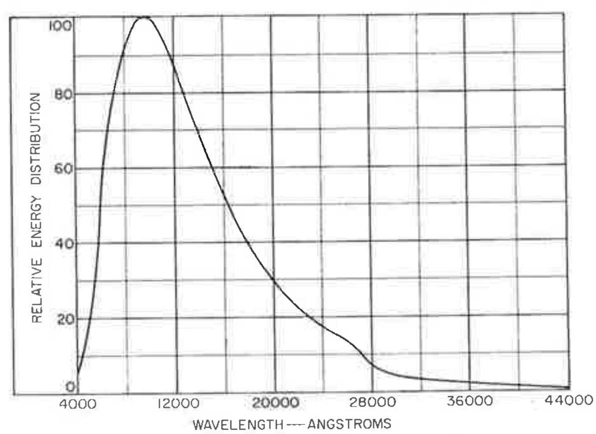

Spectral-energy emission characteristic of a tungsten-filament lamp operated at a colour temperature of 2870°K.

Voltage E (%)	Current I (%)	Power N (%)	Life (%)	Lumen (%)	Lumen/Watt (%)
150	122	184	0.51	410	225
140	118	166	1.3	325	196
130	114	148	3.3	250	169
120	109.5	131.5	9.4	189	144
110	104.9	115.9	29	139	121
105	102.5	107.6	53	119	110
100%	100%	100%	100%	100%	100%
95	97.5	92.6	195	82	90
90	94.9	85.4	390	69	81
80	89.4	71.5	1810	45	64
70	84	59	10300	28	49
60	77	47	77000	16	36

Characteristics of tungsten-filament lamps. (From ELECTRONIC DESIGN, "Light bulbs for special applications," August 19, 1959.)

Input Power Watts	Length Inches	Luminous Flux Lumens	Over-all Efficiency Lumens/Watt
4	6	73	18.2
6	9	210	35.0
8	12	330	41.2
14	15	490	35.0
20	24	960	48.0
30	36	1500	50.0
40	48	2320	58.0
100	60	4400	44.0

Overall luminous efficiency of fluorescent lamps. (From UNIVERSITY PHYSICS, Sears and Zemansky, 1955, publ. Addison Wesley.)

SUPER RADIOTRON 70-WATT HI-FI STEREO SYSTEM

More data on this interesting system, including some of the latest circuit modifications and other material.

Following the great and gratifying success of and interest in this system since it was first demonstrated to the Sydney Division of the Institution of Radio Engineers, Australia, some further work has been done preparatory to building the integrated unit which has been promised for these pages. A number of small circuit changes have resulted from this work, and these are detailed below.

Further demonstrations on the equipment have also been given, following requests from the Melbourne and Adelaide Divisions of the I.R.E. Aust. The equipment was transported to Melbourne and Adelaide during June, and demonstrated in those cities. A number of private demonstrations have also been conducted for selected groups, and more are likely at a later date.

The enormous success of this system developed for these pages has been a great encouragement to all concerned, and augurs well for future activity of a like nature. It has now been shown beyond all doubt that transistors have a place in high fidelity. It has also shown that Australia can produce work which will stand comparison with that being done anywhere.

Circuit Changes

The circuit changes of which advice can be given at this time are enumerated below, and refer to the circuit of the main amplifier, as published in the February, 1963, copy of this magazine, on page 33.

1. The values of the two 200-ohm resistors in the bias chain of the output stage have been changed to 220 ohms to bring them into line with standard values.

Page 166, please

Lens Formulas

Principal Focus

$$\frac{1}{\mu_1} = \frac{n-1}{r_2} - \frac{\mu_o\left[\,n(n-1)\,\right] - nr_1}{\mu_o\left[t(n-1)-nr_1\right] - tr_1}$$

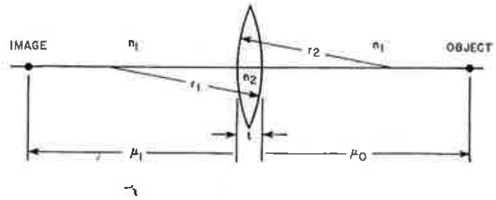

The arrowheads indicate positive values in formulas.

where

n_1 = index of refraction of medium in which object and image lie

n_2 = index of refraction of lens medium

$n = \frac{n_2}{n_1}$

r_1, r_2 = radii of curvature of lens

μ_1 = lens to image distance in image space

μ_o = lens to object distance in object space

t = thickness of lens

Material	Index of Refraction
Air	1.00
Hard Crown Glass	1.517
Dense Flint Glass	1.621

Use of formula in special cases:

For thin lenses, set t = o

For thick lenses, set $\mu_o \to \infty$ to find principal focus in image space. This gives the focal length of the lens.

For thick lenses, set $\mu_1 \to \infty$ to find principal focus in object space.

Magnification of Lens

$$M = \frac{-\mu_1\, n\, r_1}{t\,(\mu_o + r_1) - \mu_o n\,(t - r_1)}$$

A negative value indicates an inverted image.

Light and Wavelength Units Used in Photocell Measurements and Ratings

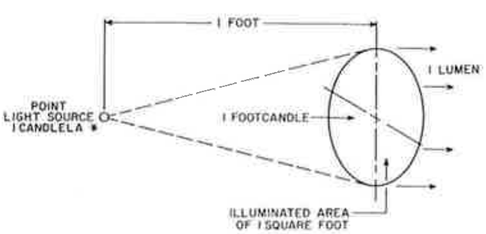

$$\text{Illumination in footcandles} = \frac{\text{Luminous Intensity in candelas}}{(\text{Distance in feet})^2} = \frac{\text{Light Flux in lumens}}{\text{Area in square feet}}$$

A light source of 1 candela emits 4π lumens.

1 Angstrom = 10^{-8} Centimeters

10^4 Angstroms = 1 Micron = 1000 Millimicrons

*The candela is defined by international agreement effective January 1, 1948.

CIRCUIT FACTOR CHARTS FOR USE WITH SILICON CONTROLLED RECTIFIERS

BY B. J. ROMAN AND J. M. NEILSON

Introduction

This article describes the design considerations for using controlled rectifiers in half-wave, full-wave bridge (two legs controlled), and three-phase half-wave rectifier circuits. Charts are included to give device current ratios as functions of conduction angles and firing angle. Also included are the voltage waveforms appearing in each described circuit and a chart showing the per cent. ripple in load voltage or current as a function of angles. A typical silicon controlled rectifier is shown in Figure 1.

General Information

Curves included in this article give ratios relating average current (I_{avg}), rms current (I_{rms}), peak current (I_{pk}), and the quantity I_o, the "reference current". I_o is a constant of the circuit equal to the peak source voltage divided by the load resistance ($I_o = V_{pk}/R_L$). I_{pk} is the current through the SCR during its period of conduction. I_o is the maximum value of current, i.e., corresponding to the peak of the sine wave. I_{pk} is identical with I_o for conduction angles greater than 90°, but is less than I_o for conduction angle less than 90°. These curves are useful for determining the following:

1. peak or rms current through a controlled rectifier when it is desired to deliver a certain average current to a load during a specific part of the conduction angle,

Fig. 1—Typical silicon controlled rectifier.

2. the necessary period of conduction if it is desired to maintain a specified peak-to-average current ratio in a particular controlled rectifier application,
3. general circuit characteristics such as average current, peak current, or rms current as functions of conduction angle for a given SCR circuit,
4. rms current at various conduction angles when it is desired to calculate power delivered to a load, or power losses in transformers, motors, leads, bus bars, fuses, etc.,
5. ratios of load current and voltage,
6. ripple percentage.

General procedures for using these curves (Figures 5 through 10) are as follows :

1. Determine which quantity (θ_c, I_o, I_{avg}, I_{avg}/I_{rms}, etc.), is desired.
2. Determine which quantities are fixed by circuit specifications.
3. Use the appropriate curve for finding the quantity in question as a function of two of the fixed quantities.

Applications

This section deals with the application of the curves of Figures 5 through 10 in specific circuit designs.

Half-Wave SCR Circuit

In this application, a 2N685 controlled rectifier is being used in a half-wave circuit to control power from a sinusoidal ac source of 120 volts rms into a 2·8 ohm load. See Figure 2.

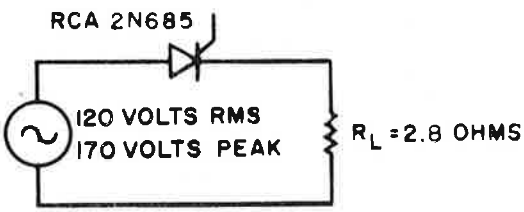

Fig. 2—Half-wave SCR circuit.

In this circuit, it is desired to have a load current which can be varied from 2 to 25 amperes rms. The problem here is to find the range of conduction angles needed to obtain this current range.

The first step is to calculate the reference current (I_o).

$$I_o = \frac{V_{pk}}{R_L} = \frac{170}{2{\cdot}8} = 61 \text{ amperes}$$

The next step is to calculate the ratios of I_{rms}/I_o for the maximum and minimum current requirements.

$$\frac{I_{rms}}{I_o} \text{ min.} = \frac{2}{61} = {\cdot}033$$

$$\frac{I_{rms}}{I_o} \text{ max.} = \frac{25}{61} = {\cdot}41$$

In the third step, corresponding conduction angles are found from curve (3) of Figure 5 by using the ratios of step 2 above.

θ_c min. = 15°, θ_c max. = 106°

Full-Wave Bridge, Two Legs Controlled

In this application, two 2N1843 controlled rectifiers are being used in a full-wave bridge as shown in Figure 3.

Here, it is desired to maintain load current at a constant value of 7 amperes average while the load resistance varies from 0·2 to 4·0 ohms. The problem here is to find the variation in conduction angle required. Average device current in this circuit will be 3·5 amperes ; one-half the load current. Device waveforms are shown in Figure 7b, current ratios in Figure 5. Waveforms for other full-wave circuits with two legs controlled are shown in Figures 7c and 7d. Waveforms for full-wave circuits with controlled load are shown in Figures 7e and 7f. Output waveforms for all full-wave circuits shown, are plotted in Figure 7a.

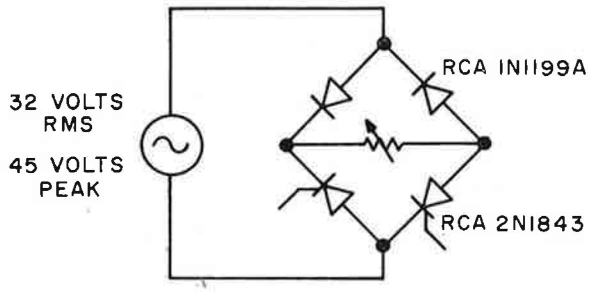

Fig. 3—Full-wave bridge, two legs controlled.

Again, the first quantity to calculate is the reference current. In this circuit, reference current will vary with load resistance. Therefore, both a maximum and a minimum are calculated.

$$I_o \text{ max.} = \frac{V_{peak}}{R_{L\ min.}} = \frac{45}{0{\cdot}2} = 225 \text{ amperes}$$

$$I_o \text{ min.} = \frac{V_{peak}}{R_{L\ max.}} = \frac{45}{4{\cdot}0} = 11{\cdot}2 \text{ amperes}$$

Corresponding ratios of I_{avg}/I_o are calculated.

$$\frac{I_{avg}}{I_{o\ max.}} = \frac{3{\cdot}5}{225} = {\cdot}015$$

$$\frac{I_{avg}}{I_{o\ min.}} = \frac{3{\cdot}5}{11{\cdot}2} = {\cdot}312$$

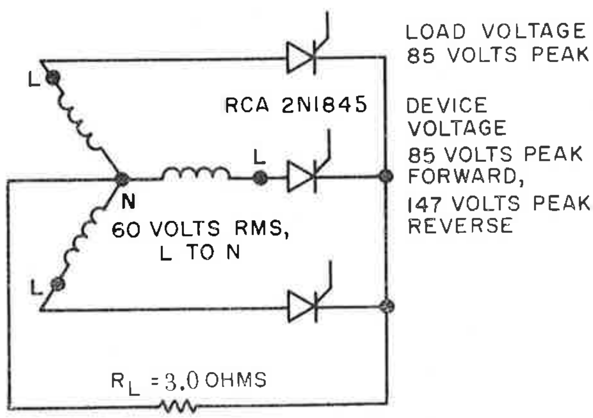

Fig. 4—Three-phase, half-wave SCR circuit.

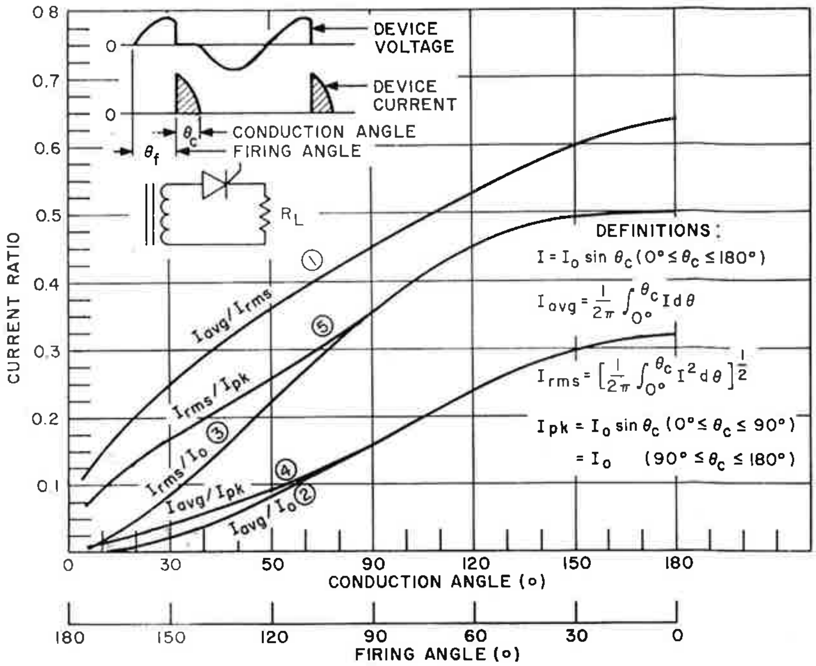

Fig. 5—SCR current ratios for single-phase, half-wave conduction with resistive load.

Conduction angles are obtained by using these ratios on curve (2) of Figure 5.

$$\theta_{c\,min.} = 25°, \ \theta_{c\,max.} = 165°$$

Three-Phase Half-Wave SCR Circuit

In the application shown in Figure 4, three 2N1845 controlled rectifiers are being used in a three-phase, half-wave SCR circuit. Firing angle can be varied continuously from 30° to 155°. The problem here is to calculate the variation in load power which can be attained.

Reference current for this circuit is as follows :

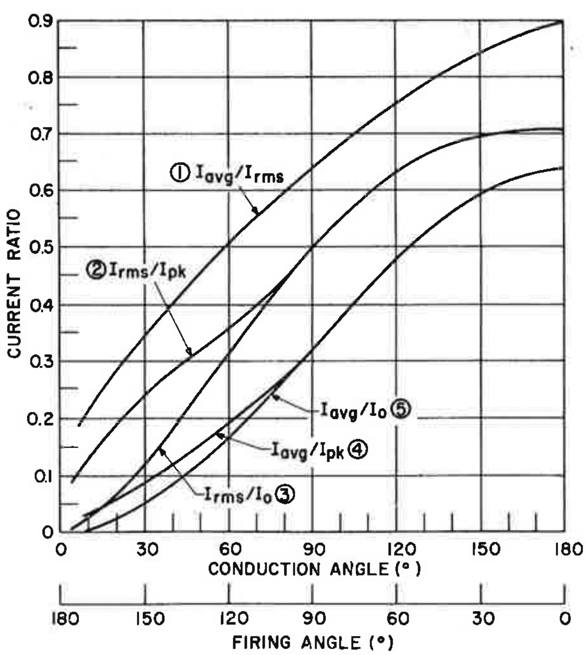

Fig. 6—SCR current ratios for single-phase, full-wave conduction with resistive load.

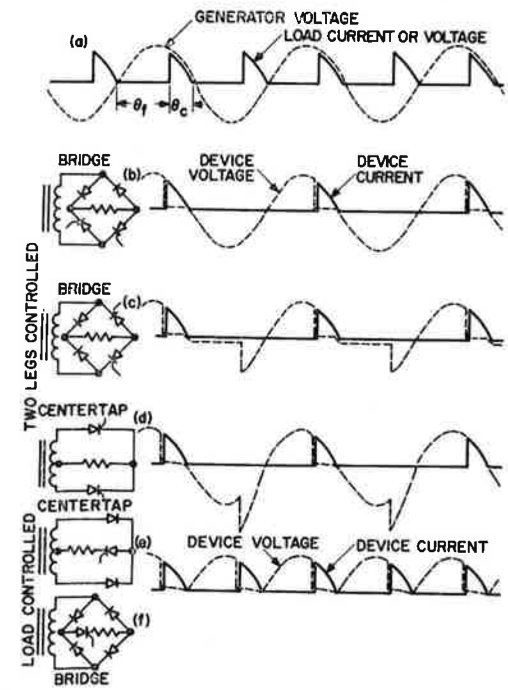

Fig. 7—Typical current and voltage waveforms for single-phase, full-wave SCR circuits with resistive loads.

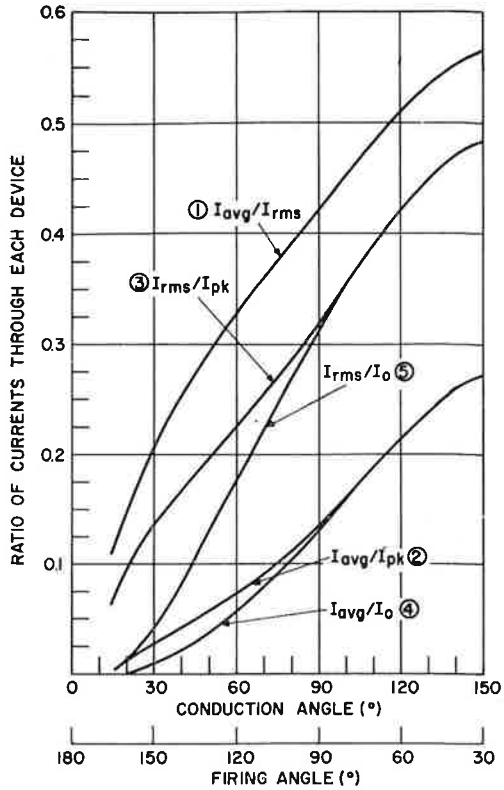

Fig. 8—SCR current ratios for three-phase, half-wave circuit with resistive load.

$$I_o = \frac{V_{L\ peak}}{R_L} = \frac{85}{3{\cdot}0} = 28 \text{ amperes}$$

Device current ratios at the extremes of the firing range are found from Figure 8. Current and voltage waveforms for silicon controlled rectifiers in three-phase, half-wave rectifier circuits are shown in Figure 9.

$$\theta_f = 30°, \frac{I_{rms}}{I_o} = {\cdot}49$$

$$\theta_f = 155°, \frac{I_{rms}}{I_o} = {\cdot}06$$

These ratios, along with the reference current, are used to find the range of rms current in the devices.

$(I_{rms\ max.}) = {\cdot}49 \times 28$ amperes $= 13{\cdot}7$ amp.
$(I_{rms\ min.}) = {\cdot}06 \times 28$ amperes $= 1{\cdot}7$ amperes

In this type of circuit, rms current in the load is—rms current multiplied by the square root of three. Therefore, load power range is found as follows :

$$P = (I_{rms}\sqrt{3})^2 R$$
$$P_{max.} = 1700 \text{ watts}$$
$$P_{min.} = 27 \text{ watts}$$

Load power therefore, can be varied continuously from 27 to 1700 watts. Per cent. of ripple in

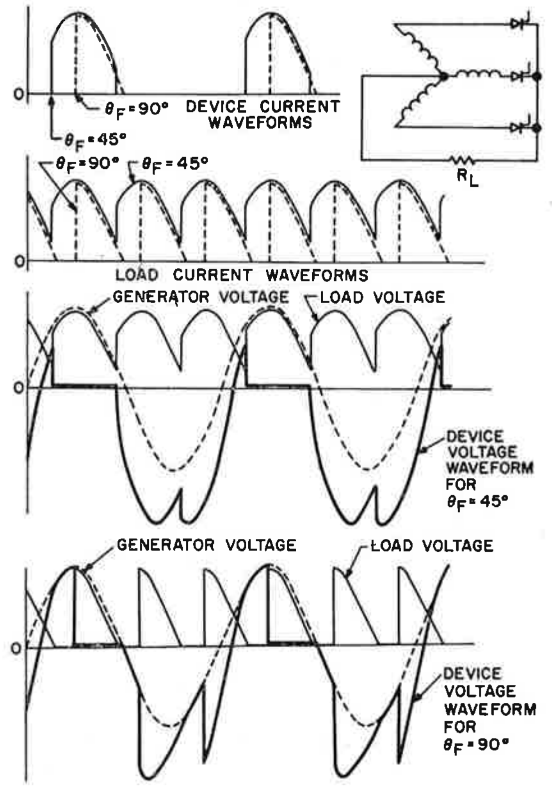

Fig. 9—Typical current and voltage waveforms for three-phase, half-wave SCR circuit with resistive load.

load current and voltage for single-phase (half-wave), single-phase (full-wave), and three-phase (half-wave) SCR circuits is plotted in Figure 10.

(With acknowledgements to RCA)

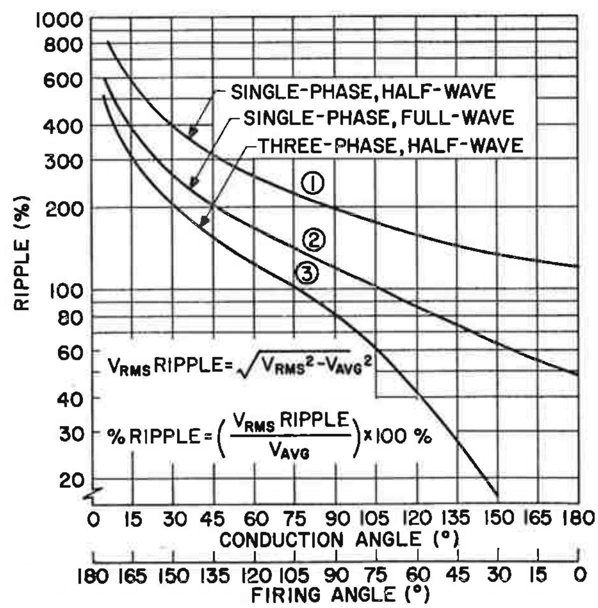

Fig. 10—Ripple expressed as a percentage in load current and voltage.

A Series on Tunnel Diodes

1: THEORY

The tunnel diode is one of the most significant electron devices to emerge from the research laboratory since the transistor. Essentially smaller and faster than either the transistor or the electron valve, it offers design engineers a host of outstanding features. The high switching speed of tunnel diodes, coupled with their simplicity and stability, makes them particularly suitable for high-speed computer applications. They can also operate effectively as amplifiers, oscillators, and converters even at microwave frequencies. In addition, tunnel diodes have extremely low power consumption and are relatively unaffected by radiation, surface effects or temperature.

The two-terminal nature of the tunnel diode is an important consideration in circuit design. On the one hand, this feature permits the design of circuits which are extremely simple, and thus provides significant savings in size and weight as well as substantial improvements in reliability. On the other hand, the lack of inherent isolation between input and output can be a serious design problem in some applications. Generally, at frequencies below the microwave region transistors are a more practical and economical choice than tunnel diodes. At microwave frequencies, however, tunnel diodes have several important advantages over transistors, and are highly competitive with other high-frequency devices such as microwave valves, parametric diodes and masers.

General Description

A **tunnel diode** is a small two-terminal device containing a single junction formed by heavily doped semiconductor materials. It differs from other p-n junction diodes primarily because the doping levels are from a hundred to several thousand times as high. For example, the doping level in conventional microwave detector diodes is in the order of 10^{16} to 10^{17} atoms per cubic centimetre, whereas the doping level in tunnel diodes is in the order of 10^{19} to 10^{20} atoms per cubic centimetre. The high impurity concentrations in both the n-type and p-type materials of tunnel diodes result in an extremely thin depletion region at the junction (approximately 0.000001 centimetre). The tunnelling effect which occurs at this junction produces the unusual current-voltage relationship and high frequency capability of the tunnel diode.

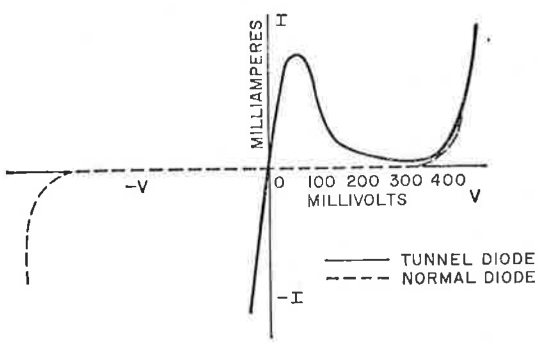

Fig. 1—Current-voltage characteristics for a tunnel diode and a conventional rectifier diode.

Fig. 1 compares the current-voltage characteristic of a tunnel diode with that of a conventional rectifier diode. In the rectifier diode, forward current does not begin to flow freely until a forward-bias voltage in the order of half a volt to a volt (depending on the semiconductor material) is applied. For conventional diodes, this forward voltage is sometimes referred to as the "offset" voltage. In the reverse-bias direction, the conventional diode has high resistance to current flow until the "breakdown" region is reached. The tunnel diode, on the other hand, is much more conductive near zero bias; appreciable current flows when small bias is applied in either the forward or reverse direction. Because the active region of tunnel diodes is at a much lower voltage than conventional devices, tunnel diodes are extremely low power devices.

As forward bias on the tunnel diode is increased, the current reaches a sharp maximum **(peak),** then drops to a deep minimum **(valley),** and finally increases exponentially with voltage as in the rectifier diode. The drop in current with increasing positive bias results in the negative-resistance characteristic of the tunnel diode. This property enables the tunnel diode to convert dc power-supply energy into an ac circuit energy, and thus permits its use as an amplifier or oscillator.

The differences in operating characteristics of conventional diodes and tunnel diodes can only be clearly explained in terms of the energy-band concept in semiconductors. The following sections describe qualitatively the theory of energy bands in semiconductors, conventional n-p junctions, and tunnel n-p junctions.

Energy Bands in Semiconductors

According to atomic theory, a single isolated atom consists of a positively charged nucleus surrounded by one or more electrons. These electrons can have only certain discrete energies. The number of electrons and the energy levels they occupy depend on the particular element, e.g., germanium has thirty-two electrons occupying four specific levels. The first three levels contain, respectively, two, eight and eighteen electrons, all of which are tightly bound to the nucleus. The fourth, and highest, energy level contains four electrons which, because of their high energy and the shielding action of the first three levels, are only loosely bound to the nucleus. In the case of germanium, it is these four electrons which generally enter into chemical reactions and which interact with other germanium atoms to form covalent bonds with adjacent atoms. These four electrons are called the valence electrons.

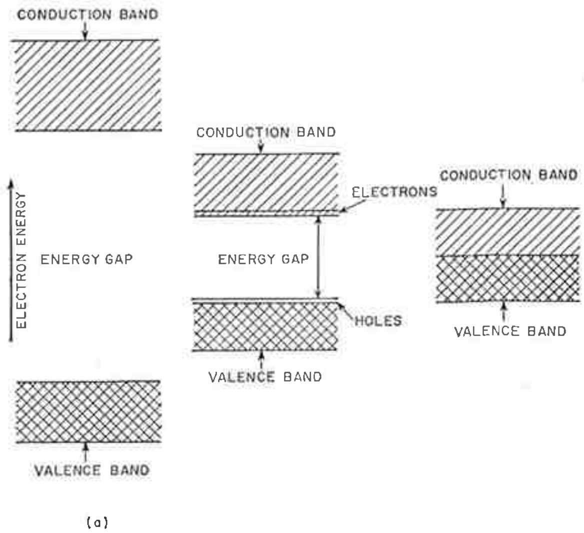

Fig. 2—Energy-band diagrams for (a) an insulator, (b) a semiconductor, and (c) a conductor.

A semiconductor is a crystalline solid in which the individual atoms occupy fixed positons in a regular pattern. Because the atoms are so closely spaced, the discrete energy levels associated with each atom merge into "bands" of allowed energies, separated by "forbidden" regions. This energy-band configuration actually determines whether a material is a semiconductor, conductor or insulator.

The energy band which contains the valence electrons is called the **valence band.** Electrons in this valence band, as well as in the higher energy bands, are not confined to any particular atom but are free to wander through the valence bands within the entire crystal. In the absence of any outside sources of energy such as thermal excitations, the valence electrons exactly fill all the possible states in the valence band. Under this idealized condition, no net current can flow, and the crystal is a perfect insulator.

The valence band is separated from the next higher band of allowed energies (the **conduction band**) by a **forbidden region;** this region is so called because it has no states for free electrons. The forbidden region between the valence band and the conduction band is called the **energy gap.** This gap represents the minimum excitation energy necessary to move an electron from the valence to the conduction band. When an electron is moved from the valence to the conduction band (e.g., through thermal excitation), the crystal is no longer an insulator. Because the conduction band has many empty states available to the free electron, the electron can now be accelerated readily by an applied field. This energy-level condition represents the basis of conduction by electrons.

At the same time, the empty state left in the valence band (as a result of the removal of an electron) permits acceleration of the valence electrons. This empty state can be considered to be a "hole," or absence of an electron in the valence band, and its effect is equivalent to that of a single positive charge. This acceleration of electrons within the valence band is called hole conduction. In general, current in a solid can be conveniently treated as motion of electrons in the conduction band and of positively charged holes in the valence band.

The width of the energy gap determines whether the solid is a semiconductor, conductor or insulator. The energy-band diagrams shown in Fig. 2 indicate the difference in band gap and free carrier concentration between an insulator, a semiconductor and a conductor material. In this figure, the ordinate represents the total energy (potential plus kinetic) of the electron, and the abscissa represents distance in one direction in the crystal.

As shown in Fig. 2a, the forbidden region of the insulator is so large that valence electrons cannot move to the conduction band except in the presence of extremely strong external energy sources; hence, the valence band remains filled and the conduction band is empty.

The semiconductor has a small enough gap so that thermal motion results in an appreciable number of electrons in the conduction band and holes in the valence band, as shown by Fig. 2b. In most semiconductor materials, the energy gap E_g ranges from a few hundredths of an electron volt to about three electron volts. For example, the energy gap for germanium is 0.7 ev, 1.1 ev for silicon, and 1.4 ev for gallium arsenide. In conductors, there is no energy gap, and the conduction and valence bands overlap, as shown in Fig. 2c. As a result, significant electron flow occurs with only a small amount of applied energy.

The discussion above concerns only pure, or intrinsic, semiconductors. In such semiconductors, every electron in the conduction band is accompanied by a corresponding hole in the valence band. However, in the case of transistors and other semiconductor devices, a large number of **free carriers** (either electrons or holes) is produced by the controlled addition of small amounts of certain impurities.

For example, if an impurity such as arsenic which contains five valence electrons is substituted for a germanium atom, only four of these electrons are used to form the covalent bond. The remaining electron is free and is readily excited into the conduction band. Instead of leaving a hole behind in the valence band (as occurs when an electron is thermally excited into the conduction band), the loss of this free electron to the conduction band ionizes the arsenic atom, i.e., the arsenic atom gives up its extra electron and becomes positively charged. Because of the small activation energy needed to ionize arsenic, practically all such **donor atoms** are ionized at room temperature. Such a material is referred to as an extrinsic **n-type** semiconductor; the energy-band diagram for such a material is shown in Fig. 3a. In the diagram, the plus signs in the valence band represent the few holes created by thermal excitation of electrons into the conduction band. As shown, the total number of electrons in the conduction band equals the sum of the donor atoms plus the holes in the valence band. As a result, the entire semiconductor crystal remains electrically neutral.

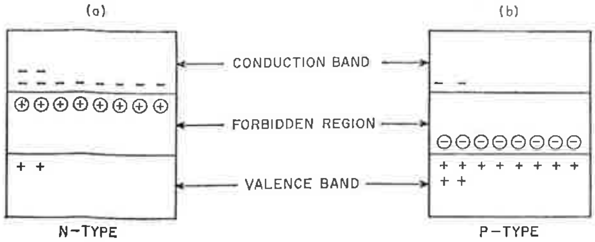

Fig. 3—Energy-band diagrams for extrinsic n-type and p-type semiconductors.

Fig. 3b shows the energy-band diagram for an extrinsic **p-type** semiconductor material, e.g., germanium doped with gallium. In this case, each impurity atom substituted for a germanium atom has one less valence electron than the germanium. The missing electron needed to complete the covalent bond is then taken from a neighbouring germanium atom. As a result, the gallium atoms acquire an extra electron, and thus become negatively ionized **(acceptor atoms).** The electrons which were used to complete the bonding leave positively charged holes behind them. The small number of electrons in the conduction band represent those electrons that acquired enough energy through thermal agitation to leave the valence band. The total number of holes in the valence band equals the sum of the acceptor atoms plus the electrons in the conduction band. As a result, the semiconductor again remains electrically neutral.

Conventional Junctions

Semiconductor p-n or n-p junctions are frequently formed by alloying or diffusing a dopant material into an oppositely doped semiconductor. For example, indium, an acceptor, can be alloyed to germanium which is doped with arsenic, a donor. Alternately, arsenic may be diffused into germanium which is doped with gallium, an acceptor. In either case, a junction is formed between the n-type and p-type regions of the semiconductor.

The current-flow mechanism across this junction is shown in Fig. 4a. This representation shows an n-type semiconductor containing a large number of donors, and a p-type containing a large number of acceptors.

The transition region from n- to p-type semiconductors consists of a dipole layer formed by immobile negatively charged acceptor atoms (not compensated by holes) and positively charged donor atoms (not neutralized by electrons). The electric field associated with this dipole layer is very high (in the order of 10,000 volts per centimetre). Because of this high field intensity, any free carriers (i.e., mobile) cannot remain in this region, but must either recombine or be swept across the junction and away from the transition region. This transition region is frequently referred to as the **depletion layer** or **space-charge region.**

Fig. 4b shows the corresponding energy-band diagram for the junction under zero-bias voltage. The energy gap E_g is the same on both sides of the junction, but the potential energy for electrons on the p-type side is increased with respect to the n-type side. The resulting **potential barrier** (E_B) results from the presence of the dipole layer of the transition region.

As a result of their random motion, some electrons approach the junction from either side. Because of the much larger number of mobile electrons on the n-type side, proportionally more electrons approach the junction from that side. If there were no potential barrier, these electrons would cross into the p-type side, until ultimately a uniform distribution of electrons would exist throughout the semiconductor. However, because of the potential barrier, only those few electrons having thermal energy greater than E_B can actually cross the junction. Thus, a small but finite current exists due to the diffusion of electrons from the n-type to the p-type material.

On the p-type side, some of the thermally generated electrons in the conduction band diffuse towards the junction. The direction of the electric field accelerates these electrons across the junction and into the n-type side. This current exactly counterbalances the diffusion current from the n-type to the p-type side; thus the net electron current is zero. The same conditions apply to the flow of holes in both directions across the

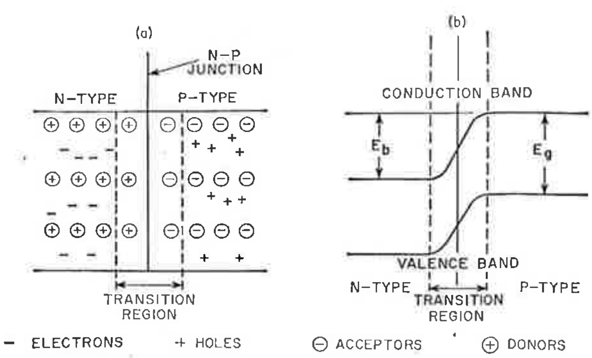

Fig. 4 — Two-dimensional representation of charges in an n-p semiconductor (a) at zero-bias voltage, and (b) corresponding energy-band diagram.

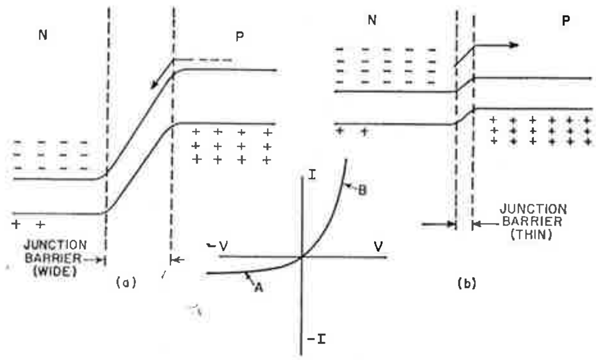

Fig. 5—Energy-band diagrams for a conventional diode under (a) reverse-bias conditions, and (b) forward-bias conditions.

junction. As a result, the net current is zero, as expected with zero applied voltage.

When a negative-bias voltage is applied to a conventional n-p junction, the energy level of electrons in the p-type material is further increased by the negative potential supplied by the voltage source. As shown in Fig. 5a, the position of the p-type energy bands is then considerably higher than that of the n-type bands. This change in energy level effectively increases the height of the junction barrier, and reduces the diffusion of electrons from the n-side across the junction to a negligible amount. Because electrons always seek the lowest energy level, the small number of electrons in the conduction band of the p-type material continue to cross the junction as before. The higher potential barrier serves to accelerate these electrons even more than for the zero-bias case. Similarly, the diffusion of holes from the p-type to the n-type side is reduced to practically zero, while the hole current from the n-type to the p-type side of the junction is not affected. The net result is a small amount of **reverse current,** as shown by point A on the current-voltage curve of Fig. 5.

Under positive-bias conditions, the height of the potential barrier is reduced, as shown in Fig. 5b. The flow of electrons from the p-type to the n-type side, and of holes from the n-type to the p-type side, remains unchanged. However, the lower potential barrier permits a larger diffusion current to flow (i.e., electrons from the n-side cross to the p-type side and holes from the p-side cross to the n-type side). Because this diffusion current is an exponential function of barrier height, even small applied voltages result in a very large **forward current,** as shown by point B on the current-voltage curve of Fig. 5.

Tunnel-Diode Junctions

As mentioned previously, tunnel diodes use much higher doping levels than conventional diode or transistor devices, and, as a result, the transition region is much narrower. Typically, the transition region in tunnel diodes is less than 100 angstroms (0.000001 centimetre), as compared with approximately 10,000 angstroms (0.0001 centimetre) for a conventional junction. This difference in width accounts for the major difference in current-flow mechanism betwen tunnel diodes and conventional semiconductor devices.

According to the laws of classical physics, an electron cannot penetrate a potential barrier. It can only "climb over" the barrier if its energy is greater than that of the barrier. This concept governs the flow of current across a conventional junction. However, the theory of quantum mechanics has shown that there is a small but finite probability that an electron having insufficient energy to climb the potential barrier can, nevertheless, penetrate it if the barrier is sufficiently narrow. Moreover, the electron has the same energy after passing through the barrier as it did before. This phenomenon, which is called **"tunnelling,"** is the basic mechanism governing the flow of current for most of the voltage range of interest in circuit applications of tunnel diodes.

Fig. 6a shows the energy-band diagram for a tunnel-diode junction under zero-bias conditions. The cross-hatched regions represent those energy states in the conduction and valence bands which are occupied by electrons. The horizontal dashed line indicates the level to which the energy states

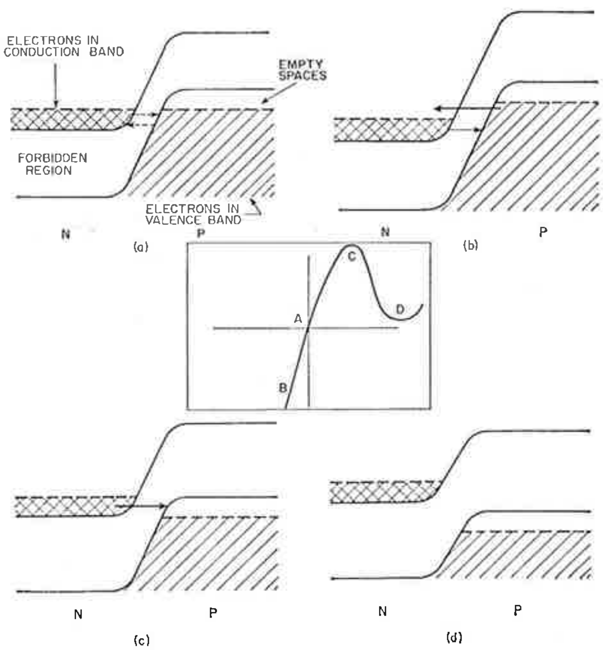

Fig. 6—Energy-band diagrams for an n-p tunnel diode junction at (a) zero-bias voltage, (b) reverse-bias voltage, (c) peak voltage, and (d) valley voltage.

on both sides of the junction are occupied by electrons. At zero applied voltage, this horizontal line is continuous, as shown. Conduction-band electrons from the n-type side can then tunnel into the p-type valence band, and the valence-band electrons from the p-type side can tunnel into the conduction band. The magnitude of these two current components is indicated in Fig. 6a by the dashed arrows across the junction. Because these components exactly balance each other at zero bias, the net current is zero.

When a reverse bias is applied, all energy levels on the p-type side are increased in relation to those of the n-type side, as shown in Fig. 6b. Because there are then many available states on the n-side facing the electrons in the p-type valence band, a large current of electrons can easily flow from the p-type to the n-type side. This heavy reverse flow is indicated by the large arrow in the diagram. The current flowing from the n-type to the p-type side remains the same as in Fig. 6a.

The tunnelling phenomenon depends exponentially on the electric field across the barrier (approximately the total barrier height divided by the transition region width divided by the electronic charge). As a result, the reverse current increases very rapidly for even small voltages. In addition, because the supply of electrons in the p-type valence band is so large, and because of the large supply of available empty states in the n-type conduction band facing the electrons, the tunnel diode is highly conductive for all values of reverse bias (see Fig. 1).

For small forward-bias voltages, the energy level of the p-type side is decreased in relation to the n-side as shown in Fig. 6c. In this case the n-type conduction-band electrons are opposite unoccupied states in the p-type valence band, while the p-type valence-band electrons are shown opposite the forbidden energy gap of the n-type side. The conduction-to-valence band current thus remains the same as in Fig. 6a, whereas the current flowing in the opposite direction is reduced to zero; thus, current flows in the forward direction.

When the forward voltage is increased further, some conduction band electrons on the n-type side are opposite the forbidden-energy gap of the p-type side, and the conduction-to-valence-band current is reduced. The forward current then decreases as the forward voltage increases. This current-voltage relationship accounts for the negative-resistance region of the tunnel diode. Finally, for a forward-bias voltage equal to the valley voltage, tunnelling completely ceases. The energy-band diagram for this condition is shown in Fig. 6d.

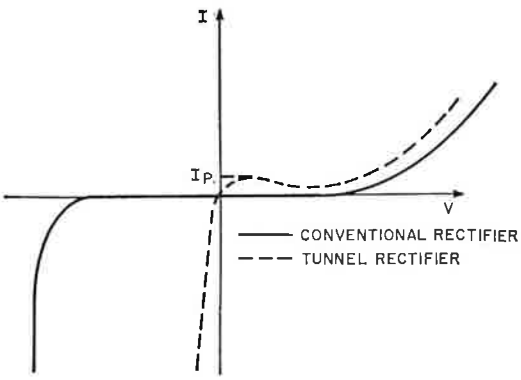

Fig. 7—Characteristics curves for a tunnel rectifier and a conventional rectifier.

Forward current flow in a tunnel diode, however, does not cease completely at the valley-voltage point, as shown in the current-voltage curve of Fig. 6. The small amount of current in this region, called **excess current,** is actually a combination of several phenomena. Some tunnelling may still occur as a result of localized impurity states (not the controlled dopant impurities) in the forbidden region. In addition, the edges of the energy-band diagram may be somewhat distorted as a result of the very high doping levels, so that the valence and conduction bands extend into the forbidden region at some points. Furthermore, tunnelling and recombination in the depletion layer produce a current component which, unlike the conventional diode current, exhibits a non-exponential dependence on temperature. At voltages greater than the valley voltage, the height of the barrier is reduced to a level which permits conventional current to flow over the barrier.

Tunnel Rectifiers

In addition to its negative-resistance properties, the tunnel diode has an efficient rectification characteristic which can be used readily in many rectifier applications. When a tunnel diode is used in a circuit in such a way that this rectification property is emphasized, rather than its negative-resistance characteristic, it is called a tunnel rectifier. In general, the peak current for a tunnel rectifier is less than one milliampere.

The major differences in the current-voltage characteristics of tunnel rectifiers and conventional rectifiers are shown in Fig. 7. In conventional rectifiers, current flow is substantial in the forward direction, but extremely small in the reverse direction (for signal voltages less than the breakdown voltage for the device). In tunnel rectifiers, however, substantial reverse current flows at very low voltages, while forward current is relatively small. Consequently, tunnel rectifiers can provide rectification at smaller signal voltages than conventional rectifiers, although their polarity requirements are opposite. (For this reason, tunnel rectifiers are sometimes called "back diodes.")

Because of their high-speed capability and superior rectification characteristics, tunnel rectifiers can be used to provide coupling in one direction and isolation in the opposite direction. More information on their applications is given in the section on Switching.

Construction and Materials

The structure of the tunnel diode is extremely simple, as shown in Fig. 8. A small dot (approximately two mils in diameter) of highly conductive n-type (or p-type) material is alloyed to a pellet of highly conductive p-type (or n-type) material to form the semiconductor junction. The pellet (approximately 0.025 inch square) is then soldered into a low-inductance, low-capacitance case. A very fine mesh screen is added to make the connection to the dot, and the junction area is reduced by etching to produce the desired peak currents. The device is then encapsulated, and a lid is welded over the cavity.

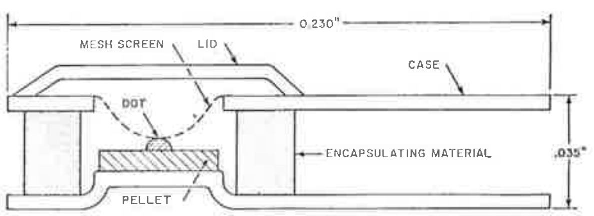

Fig. 8—Structure of a typical tunnel diode.

Tunnel-diode packages must be designed to provide both low inductance and low capacitance. This requirement immediately eliminates a large number of possible mounting and packaging approaches, including all the methods commonly used for transistors and conventional diodes. The package shown in Fig. 8 was chosen as a good compromise for both requirements; its junction area is very small, and its inductance is approximately 4 x 10^{-10} henry. This induction range is suitable for most high-frequency applications. Special packages have been developed for some microwave applications in which even lower inductances are required.

Tunnel diodes can be constructed from a variety of semiconductor materials, including germanium, silicon, gallium arsenide, indium phosphide, indium arsenide, and indium antimonide. The choice of material is a significant factor in determining the principal parameters of the device. In general, materials having small forbidden energy gaps, low effective masses, and

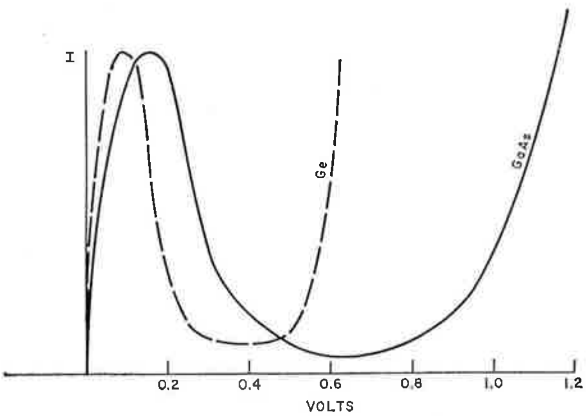

Fig. 9—Static characteristics for germanium and gallium-arsenide tunnel diodes.

low dielectric constants provide large tunnelling probabilities. These materials permit the use of small junctions and low capacitance for given peak currents, and thus provide extremely fast switching speeds.

At the present time, most commercially available tunnel diodes are fabricated from either germanium or gallium arsenide. The current-voltage characteristics of germanium and gallium arsenide tunnel diodes are compared in Fig. 9. Germanium devices offer high speed, low noise and low rise times (as low as 40 picoseconds). Gallium arsenide diodes, which have a larger voltage swing than germanium diodes, are being used in an increasing number of applications.

Indium antimonide cannot be used at normal room temperatures because of its small bandgap. Indium arsenide presents fabrication problems which make it difficult to control the desired peak-current-to-valley-current ratio. Silicon presents the same problems as indium arsenide, and also produces lower-speed devices than germanium or gallium arsenide.

(With acknowledgements to RCA)

70-WATT STEREO SYSTEM

(Continued from page 154)

2. The two 5,600 pf capacitors across the secondary windings of the driver transformer have been deleted, and replaced by a 0.001 mfd. capacitor of the ceramic variety connected across the primary of the transformer.
3. The values of the emitter resistors for Q5 and Q7 have been changed from 0.51 ohm to 0.61 ohm.
4. A 2,700 pf capacitor has been connected across the loudspeaker terminals.
5. A 2 mfd. 200 volt working capacitor has been connected between the —44 volt line and the +44 volt line, that is, across the two series-connected 500 mfd. capacitors in the power supply. This has been done for spike suppression purposes.
6. The 8,000 pf capacitor which forms part of the feedback loop from the output to the emitter of Q3 has been changed to 8,200 pf for standardisation.
7. The 22 pf and 47 pf capacitors, and the 10K and 8.2K resistors which form the feedback path from the emitter of Q2 to the base of Q1 have been deleted, and replaced by an 18K resistor with a 100 pf capacitor in parallel.
8. Values for the collector and bias resistors for Q1 should be transposed. The collector resistor should be 33K ohms, whilst the resistor between the emitter and the —35 volt line should be 18K ohms.
9. Q1 and Q2 have been changed to type 2N2613, which is a low-noise version of the same family.
10. The 1,200 mfd. electrolytic capacitor connected between the lower end of the driver transformer primary and ground has been changed to 2,000 mfd. for standardisation.

Colour Coding

There has been a number of queries regarding the colour coding of the driver transformer. The connections used are as follow:

Primary winding is blue and brown. Blue is connected to the collector of Q3, and the brown lead to the junction of the 3.3K resistor and the 2,000 mfd. capacitor.

Secondary No. 1 is red and yellow. The red lead is connected to the base of Q7, and the yellow lead to the junction of the AS15 diode and the 150-ohm resistor.

Secondary No. 2 is green and black. The green lead is connected to the base of Q5, and the black lead to the junction of the second AS15 diode and the 150-ohm resistor.

Preamplifier

A considerably modified preamplifier has been built and used for later demonstrations, partly to

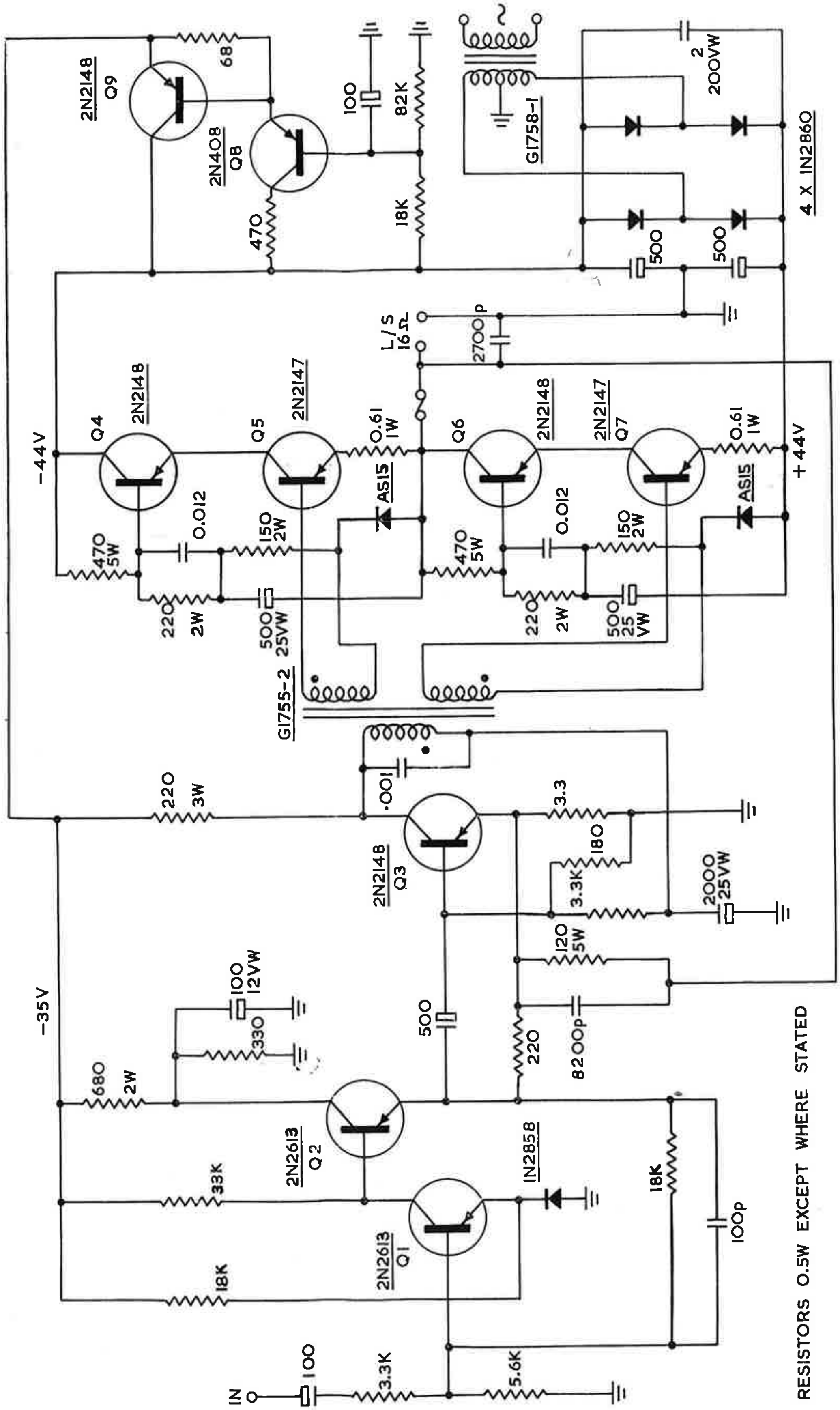
2N2148
Q9
68
2N408
Q8
470
100
82K
18K
G1758-1
2
200VW
4 X IN2860
500
500
L/S
16Ω
2700p
-44V
Q4
2N2148
Q5
2N2147
0.61
1W
Q6
2N2148
2N2147
Q7
0.61
1W
+44V
ASI5
ASI5
0.012
0.012
470
5W
150
2W
470
5W
150
2W
220
2W
500
25VW
220
2W
500
25
VW
G1755-2
220
3W
·001
3.3
180
3.3K
2N2148
Q3
2000
25VW
120
5W
-35V
100
12VW
330
500
220
8200p
680
2W
2N2613
Q2
33K
IN2858
18K
2N2613
Q1
18K
100p
IN
100
3.3K
5.6K
RESISTORS 0.5W EXCEPT WHERE STATED

use the new low-noise 2N2613 transistors. Because these transistors belong to a different family from those for which the unit was originally built, several changes in values were required. Further, in the original design, the output end of the tone control system operated at a very low level, and created a potential noise problem. The latest version has therefore been re-arranged so that we have the first two stages in very similar form, providing RIAA equalization, followed by one stage of amplification, the tone controls, and then a further stage of amplification. The emitter-follower stage in the original unit has been deleted.

The original intention with the emitter-follower stage was to use it as a point at which a high-impedance input point could be incorporated. This has proved undesirable in practice, and a number of alternatives are under consideration. Because the 35-watt amplifiers require a maximum input level from the preamplifier of only about 300 millivolts, this is all that was provided from the unit. However, in order to render the preamplifier suitable for a number of other projects, it is now being re-arranged to provide a high-level output as an alternative. Details of the preamplifier in its new form will be published as soon as tests are completed.

Other Changes

The additional work done on the units has resulted in some general improvement in performance. The improvements, however, as one may expect from the specifications already published, are small. Further, a complete re-test and re-evaluation of the unit will be required when the integrated version is completed, so it has been decided to withhold these figures until a complete specification on the integrated unit is available.

It is obvious that a notable reduction in size will be possible in the integrated version. Some of this fact arises from the ability, now that the design is established, to compact the mechanical layout. It is also clear that the very large heat sinks used in the original design can be reduced in size, particularly if the amplifier is only required to handle programme material. The large heat sinks were used as a precautionary measure at the outset as it was realised that the extended testing of the units that would be required would involve running for long periods fully driven with continuous sine wave input. This condition, as most readers will be aware, is something in the order of five times more severe on the amplifier than operation at full output with programme material.

A further saving will result from the fact that only one power supply will be required. All the elements of one of the power supplies, with the exception of the mains transformer, are quite capable of running a complete integrated stereo system. It will thus be seen that apart from the saving in size, which is perhaps not after all a very important point, there will also be a worthwhile saving in cost also.

Editor .... **Bernard J. Simpson**

Radiotronics is published twelve times a year by the Wireless Press for Amalgamated Wireless Valve Co. Pty. Ltd. The annual subscription rate in Australasia is £1, in the U.S.A. and other dollar countries $3.00, and in all other countries 25/-.

Subscribers should promptly notify Radiotronics, P.O. Box 63, Rydalmere, N.S.W., and also the local Post Office of any change of address, allowing one month for the change to become effective.

Printed by CLOISTER PRESS (W. Short), REDFERN, N.S.W.